LANGMUIR Article
Cite This: Langmuir 2019, 35, 12744−12753
pubs.acs.org/Langmuir

Characterization of Reverse Micelles Formulated with the Ionic-Liquid-like Surfactant Bmim-AOT and Comparison with the Traditional Na-AOT: Dynamic Light Scattering, ^{1}H NMR Spectroscopy, and Hydrolysis Reaction of Carbonate as a Probe

Nahir Dib,*[,†] R. Dario Falcone,[†] Angel Acuña,[‡] and Luis García-Río*[,‡]

[†]Instituto para el Desarrollo Agroindustrial y de la Salud (IDAS), CONICET-UNRC, Departamento de Química, Universidad Nacional de Río Cuarto, Agencia Postal # 3, CP X5804BYA Río Cuarto, Argentina

[‡]Centro Singular de Investigación en Química Biolóxica e Materiais Moleculares (CIQUS) and Departamento de Química Física, Universidade de Santiago de Compostela, 15782 Santiago, Spain

Supporting Information

ABSTRACT: The present study investigated how the presence of butylmethylimidazolium cation (bmim$^+$) alters the interfacial properties of reverse micelles (RMs) created with the ionic liquid-like surfactant 1-butyl-3-methylimidazolium 1,4-bis-2-ethylhexylsulfosuccinate (bmim-AOT), in comparison to sodium 1,4-bis-2-ethylhexylsulfosuccinate (Na-AOT) RMs, employing dynamic light scattering (DLS) and ^{1}H NMR techniques. Moreover, through the hydrolysis reaction of bis(4-nitrophenyl)carbonate inside both RMs as reaction probe, interfacial properties changes were explored in more detail. The kinetic solvent isotope effect was also analyzed. Micellar systems were formed using *n*-heptane as external nonpolar solvent and water as the polar component. According to the DLS studies, water is encapsulated inside the organized media; however, a different tendency is observed depending on the cationic component of the surfactant. For Na-AOT system, the results suggest that the micellar shapes are probably spherical, while in the case of bmim-AOT, a transition from ellipsoidal to spherical micelles could be occurring when water is added. ^{1}H NMR data show that water is structured differently when Na$^+$ cation is replaced by bmim$^+$; in bmim-AOT RMs, the interaction of water with the surfactant is weaker and the water hydrogen-bonding network is less disturbed than in Na-AOT RMs. Kinetic studies reveal that the hydrolysis reaction in bmim-AOT RMs was much more favorable in comparison to Na-AOT RMs. In addition, when water content decreases in bmim-AOT RMs, the hydrolysis reaction rate increases and the solvent isotope effect remains constant, while for Na-AOT solutions, both the reaction rate and the solvent isotope effect decrease. Our results indicate that bmim$^+$ cation would be located in the surfactant layer in such a way the negative charge density in the interface is less than that in Na-AOT RMs, and the reaction is more favorable. Additionally, as ^{1}H NMR studies reveal, the interfacial water molecules would be more available in bmim-AOT RMs to participate in the nucleophilic attack. Therefore, the present study evidences how the replacement of Na$^+$ counterion by bmim$^+$ alters the composition of the interface of AOT RMs.

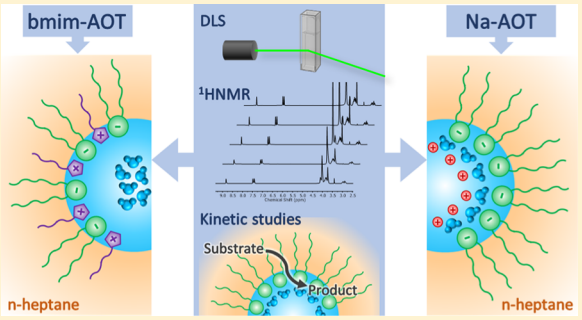

INTRODUCTION

When amphiphilic molecules (surfactants) are dissolved in different media, they can self-assemble to form diverse supramolecular systems; some examples of them are micelles, vesicles, and reverse micelles (RMs).[1] The formed system depends, among other variables, on the structure of the surfactant and the solvent used. RMs are systems typically represented by nanodroplets of a polar solvent, generally water, confined by a surfactants arrangement in a nonpolar solvent, resulting in thermodynamically stable and optically transparent solution.[2−4] In them, the surfactants are located with the polar group oriented toward the inner polar solvent, and the hydrophobic chains point toward the external nonpolar solvent. The temperature and type of external solvent and surfactant can strongly influence the amount of water solubilized (defined as W_0 = [water]/[surfactant]) in these organized systems.[4,5] RMs are widely used in different fields such as nanomaterials synthesis,[6−12] chemical and enzymatic reactions,[13−20] drug delivery,[21−26] separation science,[27,28] among others.[29,30]

Anionic, cationic, nonionic, and zwitterionic molecules have been used as surfactants to formulate RMs.[4,14,16,31−33] In this sense, one of the surfactants most employed for preparing anionic RMs is sodium 1,4-bis-2-ethylhexylsulfosuccinate (Na-AOT).[4,5] In particular, Na-AOT can be used to generate RMs in nonpolar solvents in the absence of a cosurfactant. In recent

Received: April 12, 2019
Revised: August 2, 2019
Published: September 7, 2019

DOI: 10.1021/acs.langmuir.9b01083
Langmuir 2019, 35, 12744−12753

years, new types of surfactants have been synthesized.[34,35] For example, surfactants with characteristics of ionic liquids (ILs-like surfactants), which present very interesting properties, have been relatively little studied.[35−38] ILs are low-melting-point salts (below 100 °C) with highly optimizable nature and exceptional properties,[35,39−42] which can be modulated by the selection of the cation and/or the anion in the synthesis procedure.[43]

Organic cations such as tetraalkylammonium,[44−48] 1-butyl-3-methylimidazolium (bmim$^+$),[49−54] or proliniumisopropylester[55] have been used in the past to change the counterion of AOT instead of Na$^+$, allowing to obtain IL-like surfactants that can form micelles[46,48,49,51] or vesicles[55] in water and RMs[50,52−54] in nonpolar solvents with different properties compared to the organized systems formed by Na-AOT. In particular, in previous work, we reported the formation of aqueous RMs with the IL-like surfactant 1-butyl-3-methylimidazolium 1,4-bis-2-ethylhexylsulfosuccinate (bmim-AOT, Scheme 1) in aromatic solvents (benzene, toluene, and chlorobenzene) and the study of its interfacial properties.[56,57] These systems were explored by dynamic light scattering (DLS) and static light scattering, ^{1}H NMR spectroscopy, and Fourier transform infrared (FT-IR) spectroscopy.[56] The results showed that bmim-AOT forms RMs in aromatic solvents and the organized systems increase their sizes with the addition of water. Also, FT-IR and ^{1}H NMR results revealed that in the RMs composed of water/bmim-AOT/aromatic solvent, the interaction of water with the surfactant is weaker than in the traditional water/Na-AOT/aromatic solvent RMs. More recently, the systems have been investigated by using molecular probes and UV−vis absorption spectroscopy to assess different interfacial properties at different water contents.[57] The solvatochromic behavior of molecular probes demonstrates that the hydrogen-bond donor capacity and interfacial polarity are lower in the system formed by bmim-AOT compared to Na-AOT. Also, those results suggest that bmim-AOT RMs interface is a less electron donor compared to Na-AOT. Moreover, NMR relaxometry[57,58] was used to analyze the molecular motion of interfacial water, finding that in bmim-AOT RMs, the water molecules are less limited to move inside the RMs compared to traditional Na-AOT RMs.[57]

There are some studies about bmim-AOT RMs created using different ILs as polar phase[50,52−54] and aqueous bmim-AOT RMs in aromatic nonpolar solvents,[56,57] in the absence of cosurfactants. Additionally, the bmim-AOT RMs formation using hydrophobic ionic liquids as nonpolar component and *n*-alcohol as cosurfactant has been reported.[59,60] Interestingly, there have been no reported studies on aqueous bmim-AOT RMs in aliphatic nonpolar solvents. Hence, the aim of the present work is to employ bmim-AOT as surfactant dissolved in the widely used nonpolar solvent *n*-heptane and water as polar component. The system formulated by the analogue surfactant Na-AOT in *n*-heptane was also explored as comparison. The generation of reverse micellar systems and the analysis of the interfacial properties were evaluated by DLS and ^{1}H NMR techniques. Also, we studied the kinetics of a reaction taking place at the micellar interface to examine the behavior of the water molecules in this region. Thus, we worked with a reaction model in which one of the reactants is water. Specifically, we studied the hydrolysis reaction of bis(4-nitrophenyl)carbonate[61,62] (BNPhC, Scheme 1). As the reaction environment strongly affects the hydrolysis of BNPhC, this reaction has been used to investigate the properties of water in homogeneous medium. In addition, it has been studied in different RM systems, such as water/Na-AOT/isooctane, 1-hexanol/water/sodium dodecyl sulfate/isooctane, and 1-hexanol/water/tetradecyltrimethylammonium bromide/isooctane.[63,64]

The present results allowed determining the influence of the chemical structure of the AOT counterion on the interaction of interfacial water with the surfactant in bmim-AOT RMs, altering its properties with respect to the reverse micellar systems formed by Na-AOT.

Scheme 1. Molecular Structure of 1-Butyl-3-Methylimidazolium 1,4-Bis-2-Ethylhexylsulfosuccinate (bmim-AOT; the Hydrogen Atom Labeling Is Shown) and Bis(4-nitrophenyl)carbonate (BNPhC)

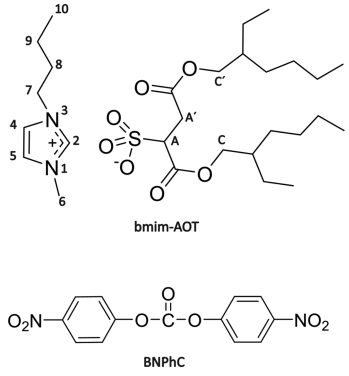

EXPERIMENTAL SECTION

Materials. The IL-like surfactant bmim-AOT was obtained following the methodology previously reported by other authors,[49] and it was dried under vacuum before use. Na-AOT, from Sigma (>99% purity), was dried at reduced pressure and then used without further purification. *n*-Heptane and deuterium oxide (D_2O), from Sigma (high-performance liquid chromatography quality), were used as supplied. The substrate BNPhC, from Sigma, was of high purity and was used without prior purification. Milli-Q (Millipore) equipment was used to obtain ultrapure water.

Methods. Experimental procedure for preparing bmim-AOT and Na-AOT RMs solutions; DLS, ^{1}H NMR, and kinetic experiments are detailed in the Supporting Information section.

RESULTS AND DISCUSSION

Water/bmim-AOT/*n*-Heptane System. As it was mentioned above, the solubilization of bmim-AOT in aromatic solvents such as benzene, toluene, and chlorobenzene in the absence of water ($W_0 = 0$) was reported.[56] In the present work, we tested the ability of bmim-AOT to form reverse micellar systems in *n*-heptane. Thus, the variation of the surfactant concentration and the water content for water/bmim-AOT/*n*-heptane system was evaluated. The concentration of bmim-AOT was varied between 0 and 1 M, and it was found that the surfactant was insoluble in *n*-heptane at $W_0 = 0$ in all of the surfactant concentration range evaluated. Therefore, to prepare clear solutions of bmim-AOT in *n*-heptane below 1 M, the addition of water was indispensable. A 0.7 M concentration of bmim-AOT was used to perform all of the experiments; at this concentration, bmim-AOT is soluble in a wide range of W_0 (W_0 = 2−35). Below W_0 = 2, the solubilization of the surfactant is incomplete, and at W_0 > 35, separation into two liquid phases occurs. Therefore, at high surfactant concentrations, the bmim-AOT/*n*-heptane system can disperse a

DOI: 10.1021/acs.langmuir.9b01083
Langmuir 2019, 35, 12744−12753

considerable amount of water, resulting in a clear and stable ternary mixture. Interestingly, this system can dissolve a larger amount of water than in aromatic solvents, where W_0^{max} is 5–6.[56]

The results suggest that just as the solubility of AOT changes by replacing the Na^+ counterion by $bmim^+$, the interfacial properties could be also altered; hence, in the next sections, we evaluate the behavior of this novel system, compared to water/Na-AOT/*n*-heptane.

DLS Experiments. DLS measurements were carried out for water/bmim-AOT/*n*-heptane at [surfactant] = 0.7 M and different W_0's, to determine if water is entrapped inside the organized media or if water only dissolves in the solution without any molecular organization.[4] Water/Na-AOT/*n*-heptane system, in the same experimental conditions, was also analyzed for comparison.

The apparent hydrodynamic diameters (d_{app}) for the RMs at variable W_0 are reported in Figure 1. Additionally, the values of polydispersity index (PDI) are listed in Table S1. As can be seen in Figure 1, depending on the cationic component of the surfactant, the observed tendency is different. When increasing the amount of water, an increase in the apparent hydrodynamic diameter is observed for water/Na-AOT/*n*-heptane system, which suggests that water is encapsulated and RMs are formed. The aggregates do not interact with each other and are probably spherical according to the observed linear trend and the low PDI values (Table S1).[65] This tendency is consistent with the results obtained for water/Na-AOT/*n*-heptane at lower surfactant concentration.[7]

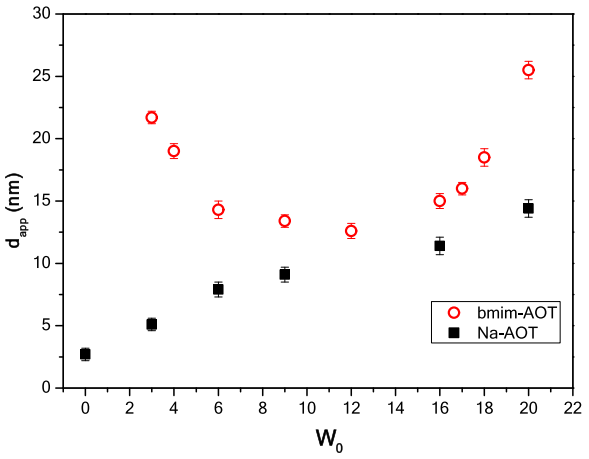

Figure 1. d_{app} values of water/bmim-AOT/*n*-heptane RMs (red circle open) and water/Na-AOT/*n*-heptane RMs (box solid) at different W_0's. Temperature = 25 °C, [surfactant] = 0.7 M.

In the case of bmim-AOT, different behavior is observed compared to Na-AOT. Figure 1 shows that d_{app} values decrease to a minimum at $W_0 \sim 12$ and then start to increase. The results suggest that a transition from ellipsoidal ($W_0 < 12$) to spherical ($W_0 > 12$) RMs could be occurring. Similar results have been found for water/sodium bis(2-ethylhexyl)phosphate (Na-DEHP)/*n*-heptane,[66,67] water/Na-DEHP/benzene,[68,69] and dimethylformamide/Na-DEHP/*n*-heptane[70] systems, which show a minimum in size when plotting d_{app} versus W_0. Beyond the changes in shape for the bmim-AOT system, the d_{app} and PDI (Table S1) values obtained confirm that the water molecules are encapsulated forming RMs. In this sense, the present work is the first investigation where an aliphatic nonpolar solvent as *n*-heptane is used as a nonpolar component to generate aqueous bmim-AOT RMs.

The d_{app} profile versus the water content for the bmim-AOT system could be analyzed taking into account the critical packing parameter (CPP).[71] The molecular structure of a surfactant is one of the factors that governs the types of molecular assemblies that are formed; this relationship is given by CPP. CPP is equal to V_c/a_0l_c, where V_c is the volume occupied by the lipophilic group of the surfactant, a_0 is the area occupied by the hydrophilic region, and l_c is the length of the lipophilic part. Surfactants in nonpolar media with CPP larger than 1 assemble in RMs;[72] an increase in a_0 decreases the CPP value so that the organized system has a less negative curvature and an elongated aggregate is expected to form.[73] In *n*-heptane, both Na-AOT and bmim-AOT form RMs; however, the IL-

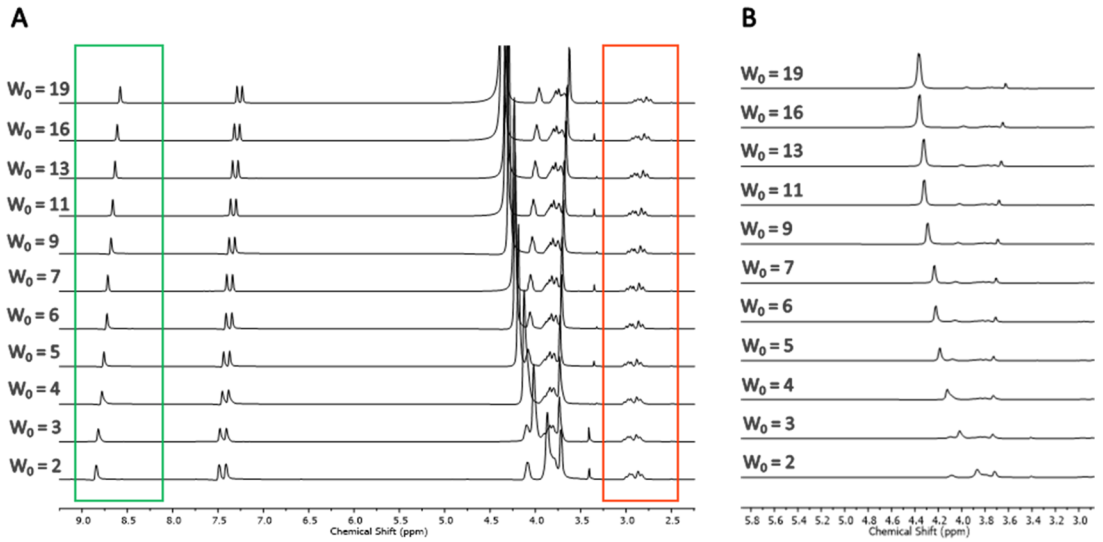

Figure 2. ^{1}H NMR spectra for water/bmim-AOT/*n*-heptane RMs obtained varying the water content at 25 °C. [bmim-AOT] = 0.7 M. (A) The lines highlight ^{1}H NMR signals of H2 from the $bmim^+$ cation (green line) and HA′ proton associated with AOT (red line). (B) ^{1}H NMR spectra in the region of 2.9–5.9 ppm showing H from water-entrapped signal.

DOI: 10.1021/acs.langmuir.9b01083
Langmuir 2019, 35, 12744–12753

like surfactant bmim-AOT has a large cation ($bmim^+$) compared to Na-AOT, which leads to a large a_0 value and lower CPP value than Na-AOT, making the formation of ellipsoidal RMs more favorable. The distance between AOT and $bmim^+$ increases when water content increases in bmim-AOT RMs due to solvation of both the anion and cation. Consequently, the a_0 value for AOT decreases and the CPP value increases, so the aggregate tends to have a more negative curvature, and the ellipsoidal RMs transform to a reverse spherical micelle. Thereby, there is a decrease in d_{app} values determined by DLS when W_0 increases, up to $W_0 < 12$. When the hydration process is complete, the micellar diameter increases for $W_0 > 12$ due to the swelling of the micelle. A similar behavior was observed by Bai et al.[50] when studying the effect of water on [bmim][BF_4]/bmim-AOT/benzene microemulsions.

^{1}H NMR Analysis. ^{1}H NMR spectroscopy is a technique that allows to analyze RM systems and to study the structure of dissolved water.[65,74−77] In the present work, ^{1}H NMR measurements in aqueous bmim-AOT RMs in *n*-heptane were carried out varying the water content (Figure 2). The chemical shift changes of hydrogen atoms of the water entrapped, HA′ proton associated with the anion AOT and H2 signal for the $bmim^+$ cation (Scheme 1) were evaluated. The ^{1}H NMR chemical shifts of the corresponding Na-AOT system were also recorded, for comparison.

Figure 3 shows the chemical shifts of H (from water) in water/bmim-AOT/*n*-heptane and water/Na-AOT/*n*-heptane RMs at different water content. The results show that in both RMs, the signal of H from water shift to a downfield position upon W_0 increase. Interestingly, the values are not identical denoting different environment around the water molecules.

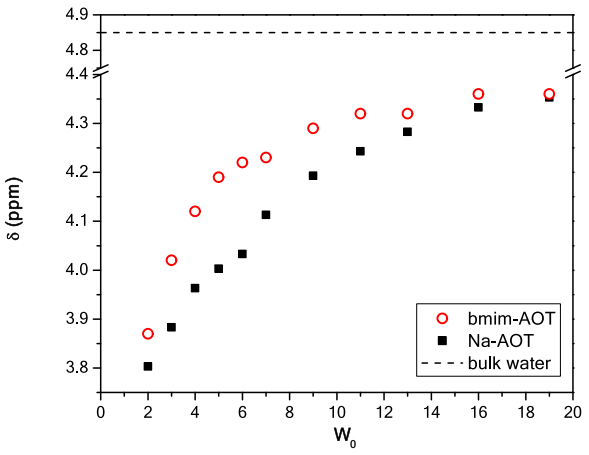

Figure 3. ^{1}H NMR chemical shifts of water hydrogen atoms in water/bmim-AOT/*n*-heptane (red circle open) and water/Na-AOT/*n*-heptane (box solid) RMs at different water content. [Surfactant] = 0.7 M. The value for bulk water (dashed line) is included.

Previous studies performed in Na-AOT RMs[76,78,79] report that as a consequence of the interaction of water with AOT polar head group, entrapped water molecules have better electron donor capability compared to bulk water. This interfacial interaction increases the electron density on water protons, whereby the chemical shifts of hydrogen atoms from entrapped water in Na-AOT RMs appear at lower value than in bulk (4.85 ppm).[76] On the other hand, the interaction of the entrapped water with positively charged counterions makes the water more electrophilic, resulting in a downfield shift in comparison to bulk water.[78,80] Therefore, at low W_0 values, most of the water present in water/bmim-AOT/*n*-heptane and water/Na-AOT/*n*-heptane RMs interacts with anionic surfactant polar head group. By increasing the amount of water in both systems, the proportion of free water progressively increases, and water begins to recover its hydrogen-bond network structure. This reduces the electron density on water protons, and the hydrogen signal moves downfield, tending to the bulk value (see the dashed line in Figure 3).

It is important to note that for bmim-AOT RMs at $W_0 < 18$, the values of water protons signal are larger than in Na-AOT RMs. For instance, the chemical shift is 4.19 ppm at $W_0 = 5$ in water/bmim-AOT/*n*-heptane RMs, while the signal appears at 4.00 ppm for Na-AOT at the same W_0. This difference is because the interaction of water with the surfactant is weaker in the bmim-AOT system than in Na-AOT RMs. In addition, when the amount of water increases, the signal trends more rapidly to the value of bulk water in bmim-AOT than in Na-AOT RMs, due to the interface solvates at low W_0.

The analysis of the AOT moiety proton signals also provides information about the interfacial properties of the micellar systems. In Figure 4A, the ^{1}H NMR signal position of HA′ proton from AOT in water/bmim-AOT/*n*-heptane RMs as a function of W_0 is shown; the signal showed upfield shift when W_0 increases. This same tendency shows the water/Na-AOT/*n*-heptane system (Figure S1). These results indicate that the sulfonate group of the surfactant interacts with the entrapped water by hydrogen bonds, thereby the spatial separation between the AOT anion and its counterion increases when W_0 increases and the proton signals from the surfactant polar head shift to an upfield position.[76]

The chemical shifts of the signal assigned to HA′ appear at lower values for bmim-AOT RMs than Na-AOT; however, the changes are more important in bmim-AOT. For example, in water/bmim-AOT/*n*-heptane RMs, the HA′ signal position changes from 2.92 ppm at $W_0 = 2$, to 2.81 ppm at $W_0 = 19$ ($\Delta\delta = 0.11$ ppm), while the signal appears at 2.97 ppm and shifts to 2.92 ppm for Na-AOT at the same W_0 range ($\Delta\delta = 0.05$ ppm). Previous studies by other authors in which the ^{1}H NMR signals of AOT polar head were analyzed varying the metal counterion indicate that if the interaction between the metal and AOT decreases, the signals of the hydrogens from surfactant polar head move upfield.[77] This allows concluding that the differences in chemical shift values of AOT HA′ proton for bmim-AOT and Na-AOT RMs are due to a weaker AOT-$bmim^+$ interaction compared to AOT-Na^+ interaction.

H2 atom in imidazolium ring in the $bmim^+$ cation (Scheme 1) is particularly sensitive to the environment;[50,81,82] therefore, the ^{1}H NMR peak position of this proton was also analyzed as a function of W_0. The signal position of the H2 of $bmim^+$ in bmim-AOT RMs at different W_0's is displayed in Figure 4B. The results show that the ^{1}H NMR peak of H2 atom shifts to a highfield position upon W_0 increase, moving from 8.84 ppm at $W_0 = 2$, to 8.58 ppm at $W_0 = 19$. This shifting indicates an increase in the electron density of H2 atom that could be attributed to water−$bmim^+$ interactions when the W_0 increases.[56]

In summary, the water addition affects more the microenvironment of bmim-AOT than Na-AOT. Consequently, the hydrogen bond and electron-donor ability of the micellar interface are altered in a dissimilar way.

DOI: 10.1021/acs.langmuir.9b01083
Langmuir 2019, 35, 12744−12753

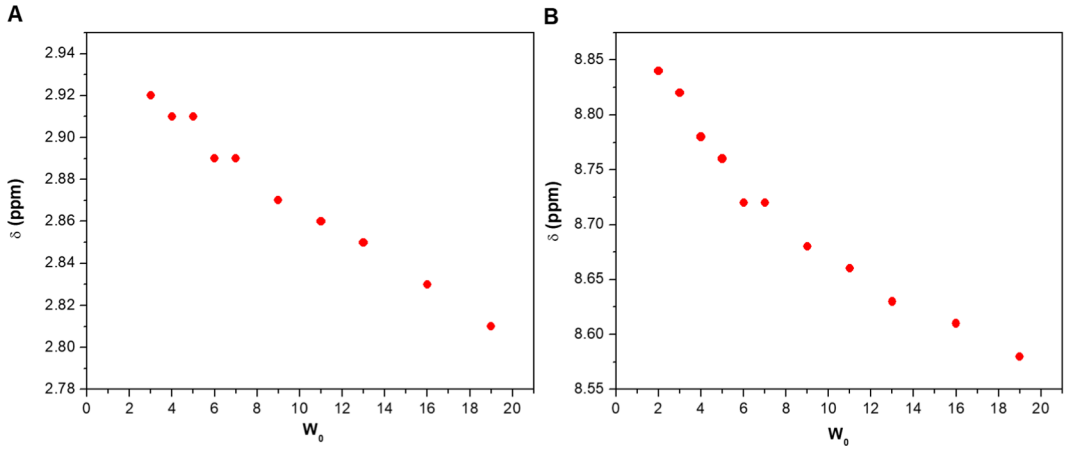

Figure 4. δ values of AOT HA′ (A) and H2 of bmim$^+$ (B) in water/bmim-AOT/*n*-heptane RMs as a function of W_0. [bmim-AOT] = 0.7 M.

Kinetic Study: Hydrolysis of Bis(4-nitrophenyl)-carbonate (BNPhC). ^{1}H NMR studies in bmim-AOT and Na-AOT RMs show that the confined water has its hydrogen-bond network partially broken as a result of the interaction of water molecules with the micellar interface. These changes in water properties strongly affect the behavior of the reactions that occur at the interface. Therefore, with the aim of studying the changes in properties of interfacial water and analyzing their influence on chemical reactivity, a model reaction in which one of the reactants is water was tested. Thus, the hydrolysis reaction of BNPhC (Scheme 2) was carried out in aqueous bmim-AOT and Na-AOT RMs using *n*-heptane as external nonpolar solvent, and the effects in reactivity at different W_0 were evaluated.

Scheme 2. Hydrolysis Reaction of BNPhC

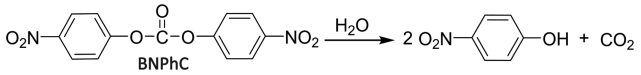

The hydrolysis of BNPhC involves one water molecule that acts as a nucleophile, attacking the carbonyl carbon atom, and another water molecule that acts as a catalytic base removing a proton (Scheme 3); thus, solvent kinetic isotope effects generally occur (usually, solvent kinetic isotope effects range from 2 to 3).[83,84]

Scheme 3. Schematic Representation of the Interaction between Water and BNPhC

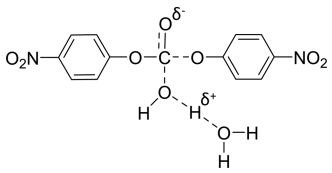

Figure S2A shows the absorption spectra of a typical run corresponding to the hydrolysis of BNPhC in RMs created with bmim-AOT. A clear isosbestic point can be observed; the band located at the shortest wavelength corresponds to BNPhC, while the product band is located at higher wavelengths. The hydrolysis reaction was followed determining the UV–vis absorbance changes of the product, at 343 nm (Figure S2B). In Na-AOT RMs, the results were similar (absorption spectra not shown).

The influence of RMs composition on the hydrolysis of BNPhC was tested by performing several experiments. The kinetic procedure to determine the observed rate constant (k_{obs}) is detailed in the Supporting Information section. The variation of k_{obs} values with [surfactant], at constant W_0 = 20, for both micellar systems was investigated. The results show an increase in k_{obs} with [surfactant] at a constant nanodrop size for both reverse micellar systems studied, due to the incorporation of BNPhC into the RMs (Figure S3). Moreover, the observed rate constants are larger for the bmim-AOT system. In addition, the k_{obs} values as function of the water content in Na-AOT and bmim-AOT reverse micellar systems at constant surfactant concentration (0.7 M) were studied, it is found that the profile of the variation of k_{obs} with W_0 is very different for bmim-AOT RMs compared to Na-AOT (Figure S4). When increasing W_0 at constant surfactant concentration, the reaction rate decreases markedly for bmim-AOT RMs, while a small increase in k_{obs} is obtained when increasing W_0 for water/Na-AOT/*n*-heptane.

For a quantitative analysis of the solvolysis reaction in RMs, we decide to use the model of the micellar pseudophase. This model considers that the micellar system consists of three pseudophases: aqueous phase, interface, and continuous medium.[2] The combination of the reaction rates in each pseudophase gives the overall reaction rate and depends on the reactant concentrations in the three pseudophases. As BNPhC is poorly soluble in water, therefore, it is assumed that it is partitioned between the oil phase ($BNPhC_o$) and the surfactant monolayer ($BNPhC_i$), whereby the reaction only takes place in the micellar interface where water and BNPhC molecules can meet to form the product (P) (Scheme 4).[64]

Taking into account the above and according to the models developed in previous works,[63,64,78] the k_{obs} values of the micellar system can be expressed by eq 1 as follows

$$k_{obs} = \frac{k_i K_{oi}}{K_{oi} + Z} \quad (1)$$

where k_i is the rate constant of hydrolysis at the micellar interface, K_{oi} is the distribution constant of BNPhC between the continuous medium and the interface, and Z is defined as Z = [*n*-heptane]/[surfactant]. Equation 1 can be rewritten as follows

DOI: 10.1021/acs.langmuir.9b01083
Langmuir 2019, 35, 12744–12753

Scheme 4. BNPhC Distribution Processes in the Micellar System and Location of the Hydrolysis Reaction[a]

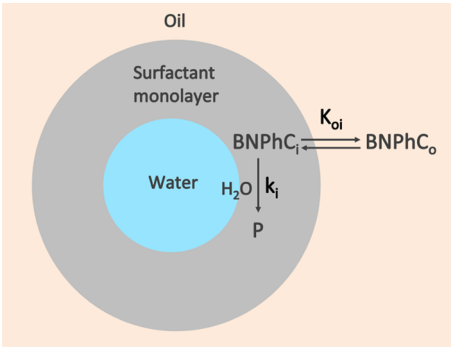

[a] K_{oi} is the distribution constant of BNPhC; k_i is the hydrolysis rate constant.

$$\frac{1}{k_{obs}} = \frac{1}{k_i} + \frac{Z}{k_i K_{oi}} \quad (2)$$

As it can be seen, eq 2 predicts that the relationship between the reciprocal of k_{obs} and Z is linear, and K_{oi} value can be obtained from the ratio between the intercept and slope.[63,78] The predicted linear relationship between $1/k_{obs}$ and Z at a constant value of W_0 was verified experimentally and K_{oi} values were obtained from the data plotted in Figure 5: K_{oi} (H_2O/Na-AOT/*n*-heptane) = 43 and K_{oi} (H_2O/bmim-AOT/*n*-heptane) = 56.

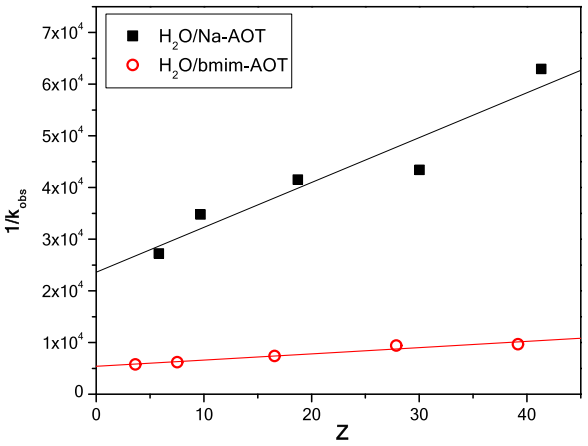

Figure 5. Reciprocal of k_{obs} for BNPhC hydrolysis plotted at different [*n*-heptane]/[surfactant] (Z) in: H_2O/Na-AOT/*n*-heptane (box solid) and H_2O/bmim-AOT/*n*-heptane (red circle open).

After determining K_{oi} and k_{obs} values at different W_0, the true rate constant at the micellar interface, k_i, at different amount of water is obtained from eq 2. For water/bmim-AOT/*n*-heptane solutions, an increase in k_i with decreasing W_0 is obtained for BNPhC hydrolysis (Figure 6A). Furthermore, a constant solvent isotope effect for bmim-AOT RMs can be observed from Figure 7. The isotope effect is defined as k_{iH}/k_{iD}, where k_{iH} and k_{iD} are the hydrolysis rate constants in the micellar interface using H_2O and D_2O, respectively. Different results were obtained for water/Na-AOT/*n*-heptane system, which shows a decrease in k_i with decreasing W_0 (Figure 6B) and a decrease in the solvent isotope effect with decreasing W_0 (Figure 7). Also, for Na-AOT RMs solutions, the hydrolysis was slower than that in the system formed by the IL-surfactant.

Previous kinetics studies[63] of the solvolysis of BNPhC in water/Na-AOT/isooctane micellar systems, as for Na-AOT/*n*-heptane, showed a decrease in the k_i values and the solvent isotope effect with decreasing W_0. Decrease in the availability and basicity of water for catalysis at the interface was suggested as an explanation. At low W_0 values, the interfacial water is solvating the surfactant and under this scenario, there are no water molecules to catalyze the nucleophilic attack (Scheme 3).

Taking into account the more hydrophobic character of $bmim^+$ in comparison with Na^+, in bmim-AOT RMs we suggest that the cation $bmim^+$ is part of the surfactant layer, hence, the negative charge density in the interface should be less than that in Na-AOT RMs. Therefore, the electrostatic repulsion with the anionic intermediate of the associative mechanism[63,85] for BNPhC hydrolysis is lower, and the reaction in bmim-AOT RMs is more favorable. Additionally, the cation $bmim^+$ can stabilize the unstable tetrahedral intermediate leading to larger reaction rates. Simultaneously, as revealed by the ^1H NMR results, in bmim-AOT RMs, smaller amount of water molecules are hydrating the surfactant, thus they are more accessible to participate in the nucleophilic attack. The fact that the rate constant of solvolysis reaction decreases at larger W_0 for bmim-AOT RMs is the result of a decreased water nucleophilicity.

Furthermore, the fact that the isotope effect in bmim-AOT RMs is around 1 for all W_0 values analyzed, could indicate the stabilization of the intermediate by the cation $bmim^+$, creating an environment less necessary for catalytic participation of the second water molecule.

Therefore, our results show that changing the chemical structure of the counterion on the AOT surfactant generates a new system with different interactions between water molecules and micellar interface and consequently with interesting properties and reactivity.

CONCLUSIONS

The IL bmim-AOT was evaluated as a surfactant to generate RMs in *n*-heptane and was analyzed on how the $bmim^+$ cation alters the properties of water/bmim-AOT/*n*-heptane RMs compared to the water/Na-AOT/*n*-heptane system. The results show that bmim-AOT form RMs and the reverse micellar system generated by this IL-surfactant has the ability to dissolve a considerable amount of water.

In particular, DLS studies reveal that water is encapsulated by forming RMs; however, taking into account the cationic component of the surfactant, a different tendency on the sizes is observed. For Na-AOT system, a spherical micellar shape can be invoked, while in the case of bmim-AOT RMs, a transition from ellipsoidal to spherical micelles could be occurring when water is encapsulated.

^1H NMR data show that water is structured differently when Na^+ cation is replaced by $bmim^+$, due to differences in the magnitude of the interaction between water molecules and the RMs interface. In bmim-AOT RMs, this interaction is weaker compared to Na-AOT RMs; consequently, in the bmim-AOT system, there is a smaller number of water molecules that interact with the surfactant and the hydrogen bonding network of water is more preserved.

These changes in water properties affect the behavior of reactions that occur in these aggregates. This was corroborated

DOI: 10.1021/acs.langmuir.9b01083
Langmuir 2019, 35, 12744−12753

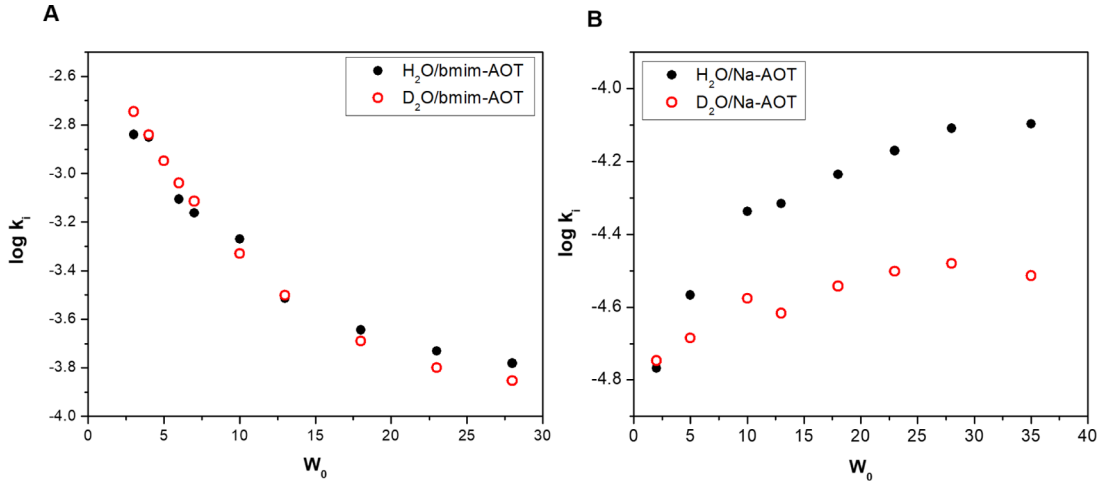

Figure 6. Log k_i values as a function of W_0 for BNPhC hydrolysis reaction in (A) H_2O (D_2O)/bmim-AOT/*n*-heptane and (B) H_2O (D_2O)/Na-AOT/*n*-heptane RMs. H_2O (circle solid) and D_2O (red circle open). [Surfactant] = 0.7 M.

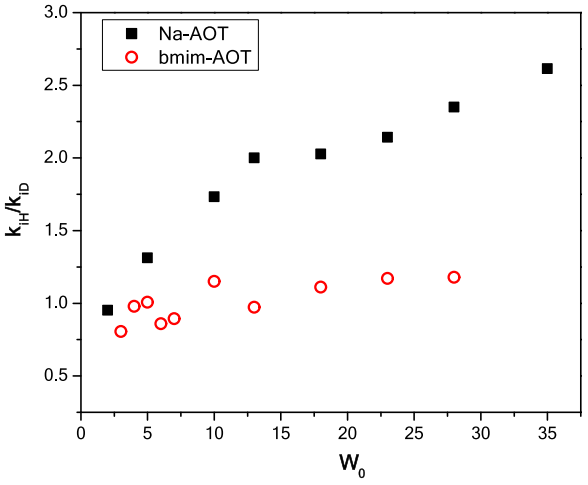

Figure 7. Variation of the kinetic isotope effect (k_{iH}/k_{iD}) vs W_0 for the hydrolysis reaction of BNPhC in aqueous Na-AOT and bmim-AOT RMs using *n*-heptane as a nonpolar component. [Surfactant] = 0.7 M.

using, as model, a hydrolysis reaction of carbonate in RM systems. In bmim-AOT RMs, the hydrolysis reaction is much more favorable compared to Na-AOT RMs. Also, for bmim-AOT solutions, an increase of reaction rate with decreasing W_0 is obtained for hydrolysis and a constant solvent isotope effect, while for Na-AOT RMs, a decrease in hydrolysis rate and solvent isotope effect with decreasing W_0 is observed. The results are compatible with an ordering of bmim-AOT surfactant at the RM interface. We think that the imidazolium ring can be inserted between the AOT moiety leading to that the negative charge density in the interface would be less than that in Na-AOT RMs, thereby the reaction is more favorable as a consequence of the lower electrostatic repulsion with the anionic intermediate of the hydrolysis. Simultaneously, as revealed by the ^{1}H NMR results, in bmim-AOT RMs, a smaller amount of water molecules are hydrating the surfactant, consequently they are more available to participate in the nucleophilic attack.

Therefore, our results show how $bmim^+$ alters the conformation of the interface of bmim-AOT reverse micelles compared to Na-AOT. The results provide kinetic evidence of these interfacial changes as a consequence of the replacement of the cation in AOT RMs.

■ ASSOCIATED CONTENT

Supporting Information

The Supporting Information is available free of charge on the ACS Publications website at DOI: 10.1021/acs.langmuir.9b01083.

Full experimental detailed procedures containing RM preparation, DLS, ^{1}H NMR, and kinetic experiments; apparent diameter (d_{app}) and polydispersity index (PDI) of water/Na-AOT/*n*-heptane and water/bmim-AOT/*n*-heptane RMs at different W_0, temperature = 25 °C, [surfactant] = 0.7 M (Table S1); ^{1}H NMR signal position of HA′ in water/Na-AOT/*n*-heptane as a function of W_0, [Na-AOT] = 0.7 M (Figure S1); (A) UV−vis spectra for BNPhC hydrolysis in RMs created with bmim-AOT in *n*-heptane at 25 °C [BNPhC] = 1×10^{-4} M, [bmim-AOT] = 0.7 M, W_0 = 20 and (B) absorbance at 343 nm vs time for the reaction (A); (circle solid) experimental data and (red line) first-order reaction fit according to eq S1 (Figure S2); k_{obs} for BNPhC hydrolysis vs [surfactant] in Na-AOT and bmim-AOT RMs using *n*-heptane as a nonpolar component, at W_0 = 20 (Figure S3); and k_{obs} for BNPhC hydrolysis vs W_0 in Na-AOT and bmim-AOT RMs using *n*-heptane as a nonpolar component, at constant surfactant concentration, [surfactant] = 0.7 M (Figure S4) (PDF)

■ AUTHOR INFORMATION

Corresponding Authors

*E-mail: ndib@exa.unrc.edu.ar (N.D.).
*E-mail: luis.garcia@usc.es (L.G.-R.).

ORCID

Nahir Dib: 0000-0001-8013-7610
R. Dario Falcone: 0000-0002-0997-3437

Notes

The authors declare no competing financial interest.

DOI: 10.1021/acs.langmuir.9b01083
Langmuir 2019, 35, 12744−12753

■ ACKNOWLEDGMENTS

The financial support from the Consejo Nacional de Investigaciones Científicas y Técnicas (PIP CONICET 112-2015-0100283), Universidad Nacional de Río Cuarto (PPI-UNRC 2016−2018), Agencia Nacional de Promoción Científica y Técnica (PICT 2012-0232, PICT 2012-0526, PICT 2015-0585), and Ministerio de Ciencia y Tecnología, Gobierno de la Provincia de Córdoba (PID 2013) is gratefully acknowledged. R.D.F. holds a research position at CONICET. N.D. acknowledges CONICET for a research fellowship. L.G.-R. and A.A. acknolwedge the Ministerio de Economia y Competitividad of Spain (project CTQ2017-84354-P), Xunta de Galicia (GR 2007/085; IN607C 2016/03 and Centro singular de investigación de Galicia accreditation 2016−2019, ED431G/09), and the European Regional Development Fund (ERDF).

■ REFERENCES

(1) Holmberg, H.; Jonsson, B.; Kronbreg, B.; Lindman, B. *Surfactants and Polymers in Aqueous Solution*, 2nd ed.; Wiley: Hoboken, 2003.

(2) Silber, J. J.; Biasutti, A.; Abuin, E.; Lissi, E. Interactions of small molecules with reverse micelles. *Adv. Colloid Interface Sci.* **1999**, *82*, 189−252.

(3) Langevin, D. Micelles and microemulsions. *Annu. Rev. Phys. Chem.* **1992**, *43*, 341−369.

(4) Correa, N. M.; Silber, J. J.; Riter, R. E.; Levinger, N. E. Nonaqueous polar solvents in reverse micelle systems. *Chem. Rev.* **2012**, *112*, 4569−4602.

(5) De, T. K.; Maitra, A. Solution Behaviour of Aerosol OT in Non-Polar Solvents. *Adv. Colloid Interface Sci.* **1995**, *59*, 95−193.

(6) Naoe, K.; Yoshimoto, S.; Naito, N.; Kawagoe, M.; Imai, M. Preparation of protein nanoparticles using AOT reverse micelles. *Biochem. Eng. J.* **2011**, *55*, 140−143.

(7) Gutierrez, J. A.; Falcone, R. D.; Lopez-Quintela, M. A.; Buceta, D.; Silber, J. J.; Correa, N. M. On the Investigation of the Droplet-Droplet Interactions of Sodium 1,4-Bis(2-ethylhexyl) Sulfosuccinate Reverse Micelles upon Changing the External Solvent Composition and Their Impact on Gold Nanoparticle Synthesis. *Eur. J. Inorg. Chem.* **2014**, *2014*, 2095−2102.

(8) López-Quintela, M. A.; Tojo, C.; Blanco, M. C.; Rio, L. G.; Leis, J. R. Microemulsion dynamics and reactions in microemulsions. *Curr. Opin. Colloid Interface Sci.* **2004**, *9*, 264−278.

(9) Orellano, M. S.; Porporatto, C.; Silber, J. J.; Falcone, R. D.; Correa, N. M. AOT reverse micelles as versatile reaction media for chitosan nanoparticles synthesis. *Carbohydr. Polym.* **2017**, *171*, 85−93.

(10) Yi, S.; Dai, F.; Zhao, C.; Si, Y. A reverse micelle strategy for fabricating magnetic lipase-immobilized nanoparticles with robust enzymatic activity. *Sci. Rep.* **2017**, *7*, No. 9806.

(11) Yi, M.; Park, S. K.; Seong, C. Y.; Piao, Y.; Yu, T. The general synthesis and characterization of rare earth orthovanadate nanocrystals and their electrochemical applications. *J. Alloys Compd.* **2017**, *693*, 825−831.

(12) Sargazi, G.; Afzali, D.; Mostafavi, A. A novel synthesis of a new thorium (IV) metal organic framework nanostructure with well controllable procedure through ultrasound assisted reverse micelle method. *Ultrason. Sonochem.* **2018**, *41*, 234−251.

(13) Moyano, F.; Setien, E.; Silber, J. J.; Correa, N. M. Enzymatic hydrolysis of N-benzoyl-l-tyrosine p-nitroanilide by α-chymotrypsin in DMSO-water/AOT/n-heptane reverse micelles. A unique interfacial effect on the enzymatic activity. *Langmuir* **2013**, *29*, 8245−8254.

(14) Moyano, F.; Falcone, R. D.; Mejuto, J. C.; Silber, J. J.; Correa, N. M. Cationic Reverse Micelles Create Water with Super Hydrogen-Bond-Donor Capacity for Enzymatic Catalysis: Hydrolysis of 2-Naphthyl Acetate by α-Chymotrypsin. *Chem. − Eur. J.* **2010**, *16*, 8887−8893.

(15) Durantini, A. M.; Falcone, R. D.; Silber, J. J.; Correa, N. M. Effect of Confinement on the Properties of Sequestered Mixed Polar Solvents: Enzymatic Catalysis in Nonaqueous 1,4-Bis-2-ethylhexylsulfosuccinate Reverse Micelles. *ChemPhysChem* **2016**, *17*, 1678−1685.

(16) Blach, D.; Pessêgo, M.; Silber, J. J.; Correa, N. M.; García-Río, L.; Falcone, R. D. Ionic liquids entrapped in reverse micelles as nanoreactors for bimolecular nucleophilic substitution reaction. Effect of the confinement on the chloride ion availability. *Langmuir* **2014**, *30*, 12130−12137.

(17) García-Río, L.; Hervella, P.; Rodríguez-Dafonte, P. Solvolysis of benzoyl halides in water/NH_4DEHP/isooctane microemulsions. *Langmuir* **2006**, *22*, 7499−7506.

(18) Garcia-Rio, L.; Leis, J. R.; Pena, M. E.; Iglesias, E. Transfer of the nitroso group in water/AOT/isooctane microemulsions: intrinsic and apparent reactivity. *J. Phys. Chem. A* **1993**, *97*, 3437−3442.

(19) Mitsou, E.; Xenakis, A.; Zoumpanioti, M. Oxidation catalysis by enzymes in microemulsions. *Catalysts* **2017**, *7*, No. 52.

(20) Pogrzeba, T.; Schmidt, M.; Milojevic, N.; Urban, C.; Illner, M.; Repke, J. U.; Schomäcker, R. Understanding the Role of Nonionic Surfactants during Catalysis in Microemulsion Systems on the Example of Rhodium-Catalyzed Hydroformylation. *Ind. Eng. Chem. Res.* **2017**, *56*, 9934−9941.

(21) Kogan, A.; Garti, N. Microemulsions as transdermal drug delivery vehicles. *Adv. Colloid Interface Sci.* **2006**, *123−126*, 369−385.

(22) Müller-Goymann, C. C. Physicochemical characterization of colloidal drug delivery systems such as reverse micelles, vesicles, liquid crystals and nanoparticles for topical administration. *Eur. J. Pharm. Biopharm.* **2004**, *58*, 343−356.

(23) Callender, S. P.; Mathews, J. A.; Kobernyk, K.; Wettig, S. D. Microemulsion utility in pharmaceuticals: Implications for multi-drug delivery. *Int. J. Pharm.* **2017**, *526*, 425−442.

(24) Singh, Y.; Meher, J. G.; Raval, K.; Khan, F. A.; Chaurasia, M.; Jain, N. K.; Chourasia, M. K. Nanoemulsion: Concepts, development and applications in drug delivery. *J. Controlled Release* **2017**, *252*, 28−49.

(25) Ita, K. Progress in the use of microemulsions for transdermal and dermal drug delivery. *Pharm. Dev. Technol.* **2017**, *22*, 467−475.

(26) Nastiti, C.; Ponto, T.; Abd, E.; Grice, J.; Benson, H.; Roberts, M. Topical Nano and Microemulsions for skin delivery. *Pharmaceutics* **2017**, *9*, No. 37.

(27) Watarai, H. Microemulsions in separation sciences. *J. Chromatogr. A* **1997**, *780*, 93−102.

(28) Prabhu, A.; Chityala, S.; Garg, Y.; Venkata Dasu, V. Reverse micellar extraction of papain with cationic detergent based system: an optimization approach. *Prep. Biochem. Biotechnol.* **2017**, *47*, 236−244.

(29) Paul, B. K.; Moulik, S. P. Uses and applications of microemulsions. *Curr. Sci.* **2001**, *80*, 990−1001.

(30) Eastoe, J.; Gold, S.; Rogers, S.; Wyatt, P.; Steytler, D. C.; Gurgel, A.; Heenan, R. K.; Fan, X.; Beckman, E. J.; Enick, R. M. Designed CO_2-Philes Stabilize Water-in-Carbon Dioxide Microemulsions. *Angew. Chem., Int. Ed.* **2006**, *45*, 3675−3677.

(31) Crosio, M. A.; Correa, N. M.; Silber, J. J.; Falcone, R. D. A protic ionic liquid, when entrapped in cationic reverse micelles, can be used as a suitable solvent for a bimolecular nucleophilic substitution reaction. *Org. Biomol. Chem.* **2016**, 3170−3177.

(32) Villa, C. C.; Correa, N. M.; Silber, J. J.; Falcone, R. D. Catanionic Reverse Micelles as Optimal Microenvironment to Alter the Water Electron Donor Capacity in a SN_2 Reaction. *J. Org. Chem.* **2019**, *84*, 1185−1191.

(33) Sawada, K.; Ueda, M. Enzyme processing of wool fabrics in a non-ionic surfactant reverse micellar system. *J. Chem. Technol. Biotechnol.* **2004**, *79*, 376−380.

(34) Yue, K.; Liu, C.; Guo, K.; Wu, K.; Dong, X.; Liu, H.; Huang, M.; Wesdemiotis, C.; Cheng, S. D.; Zhang, W. Exploring shape amphiphiles beyond giant surfactants: molecular design and click synthesis. *Polym. Chem.* **2013**, *4*, 1056−1067.

DOI: 10.1021/acs.langmuir.9b01083
Langmuir 2019, 35, 12744−12753

(35) Paul, B. K.; Moulik, S. P. *Ionic Liquid-Based Surfactant Science: Formulation, Characterization, and Applications*; John Wiley & Sons, 2015.
(36) Pal, A.; Yadav, A. Mixed Micellization of a Trisubstituted Surface Active Ionic Liquid 1-Dodecyl-2,3-Dimethylimidazolium Chloride [C_{12}bmim][Cl] with an Amphiphilic Drug Amitriptyline Hydrochloride AMT: A Detailed Insights from Conductance and Surface Tension Measurements. *J. Mol. Liq.* **2019**, *279*, 43−50.
(37) Liu, Q.; Lu, D.; Yao, Y.; Huang, Q.; Shi, Y.; Sun, S. Reversible Surface Activity and Self-Assembly Behavior and Transformation of Amphiphilic Ionic Liquids in Water Induced by a Pillar[5]Arene-Based Host-Guest Interaction. *J. Colloid Interface Sci.* **2018**, *533*, 42−46.
(38) Singh, G.; Singh, G.; Kang, T. S. Micellization Behavior of Surface Active Ionic Liquids Having Aromatic Counterions in Aqueous Media. *J. Phys. Chem. B* **2016**, *120*, 1092−1105.
(39) Zhang, S.; Zhang, J.; Zhang, Y.; Deng, Y. Nanoconfined ionic liquids. *Chem. Rev.* **2017**, *117*, 6755−6833.
(40) Welton, T. Ionic Liquids: A Brief History. *Biophys. Rev.* **2018**, *10*, 691−706.
(41) Austen Angell, C.; Ansari, Y.; Zhao, Z. Ionic Liquids: Past, Present and Future. *Faraday Discuss.* **2012**, *154*, 9−27.
(42) Hayes, R.; Warr, G. G.; Atkin, R. Structure and nanostructure in ionic liquids. *Chem. Rev.* **2015**, *115*, 6357−6426.
(43) Dean, P. M.; Pringle, J. M.; MacFarlane, D. R. Structural analysis of low melting organic salts: perspectives on ionic liquids. *Phys. Chem. Chem. Phys.* **2010**, *12*, 9144−9153.
(44) Revillod, G.; Nishi, N.; Kakiuchi, T. Orientation correlation of sulfosuccinate-based room-temperature ionic liquids studied by polarization-resolved hyper-Rayleigh scattering. *J. Phys. Chem. B* **2009**, *113*, 15322−15326.
(45) Lava, K.; Binnemans, K.; Cardinaels, T. Piperidinium, piperazinium and morpholinium ionic liquid crystals. *J. Phys. Chem. B* **2009**, *113*, 9506−9511.
(46) Brown, P.; Butts, C.; Dyer, R.; Eastoe, J.; Grillo, I.; Guittard, F.; Rogers, S.; Heenan, R. Anionic surfactants and surfactant ionic liquids with quaternary ammonium counterions. *Langmuir* **2011**, *27*, 4563−4571.
(47) Nishi, N.; Kawakami, T.; Shigematsu, F.; Yamamoto, M.; Kakiuchi, T. Fluorine-free and hydrophobic room-temperature ionic liquids, tetraalkylammonium bis (2-ethylhexyl) sulfosuccinates, and their ionic liquid-water two-phase properties. *Green Chem.* **2006**, *8*, 349−355.
(48) Brown, P.; Butts, C. P.; Eastoe, J.; Grillo, I.; James, C.; Khan, A. New catanionic surfactants with ionic liquid properties. *J. Colloid Interface Sci.* **2013**, *395*, 185−189.
(49) Brown, P.; Butts, C. P.; Eastoe, J.; Fermin, D.; Grillo, I.; Lee, H. C.; Parker, D.; Plana, D.; Richardson, R. M. Anionic surfactant ionic liquids with 1-butyl-3-methyl-imidazolium cations: characterization and application. *Langmuir* **2012**, *28*, 2502−2509.
(50) Bai, T.; Ge, R.; Gao, Y.; Chai, J.; Slattery, J. M. The effect of water on the microstructure and properties of benzene/[bmim]-[AOT]/[bmim][BF_4] microemulsions. *Phys. Chem. Chem. Phys.* **2013**, *15*, 19301−19311.
(51) Cheng, N.; Ma, X.; Sheng, X.; Wang, T.; Wang, R.; Jiao, J.; Yu, L. Aggregation behavior of anionic surface active ionic liquids with double hydrocarbon chains in aqueous solution: experimental and theoretical investigations. *Colloids Surf., A* **2014**, *453*, 53−61.
(52) Rao, V. G.; Ghosh, S.; Ghatak, C.; Mandal, S.; Brahmachari, U.; Sarkar, N. Designing a new strategy for the formation of IL-in-oil microemulsions. *J. Phys. Chem. B* **2012**, *116*, 2850−2855.
(53) Rao, V. G.; Mandal, S.; Ghosh, S.; Banerjee, C.; Sarkar, N. Ionic liquid-in-oil microemulsions composed of double chain surface active ionic liquid as a surfactant: temperature dependent solvent and rotational relaxation dynamics of coumarin-153 in [Py][TF_2N]/[C_4mim][AOT]/benzene microemulsions. *J. Phys. Chem. B* **2012**, *116*, 8210−8221.
(54) Rao, V. G.; Mandal, S.; Ghosh, S.; Banerjee, C.; Sarkar, N. Phase boundaries, structural characteristics, and NMR spectra of ionic liquid-in-oil microemulsions containing double chain surface active ionic liquid: a comparative study. *J. Phys. Chem. B* **2013**, *117*, 1480−1493.
(55) Srinivasa Rao, K.; Gehlot, P. S.; Trivedi, T. J.; Kumar, A. Self-assembly of new surface active ionic liquids based on Aerosol-OT in aqueous media. *J. Colloid Interface Sci.* **2014**, *428*, 267−275.
(56) Lépori, C. M. O.; Correa, N. M.; Silber, J. J.; Falcone, R. D. How the cation 1-butyl-3-methylimidazolium impacts the interaction between the entrapped water and the reverse micelle interface created with an ionic liquid-like surfactant. *Soft Matter* **2016**, *12*, 830−844.
(57) Lépori, C. M O.; Correa, N. M.; Silber, J. J.; Chávez, F. V.; Falcone, R. D. Interfacial properties modulated by the water confinement in reverse micelles created by the ionic liquid-like surfactant bmim-AOT. *Soft Matter* **2019**, *15*, 947−955.
(58) Kassab, G.; Petit, D.; Korb, J. P.; Tajouri, T.; Levitz, P. Brownian dynamics of water confined in AOT reverse micelles: A field-cycling deuteron NMR relaxometry study. *C. R. Chim.* **2010**, *13*, 394−398.
(59) Wang, R.; Feng, Z.; Jin, W.; Huang, X. Phase Behavior of the Anionic Surfactant [Bmim][AOT]-Stabilized Hydrophobic Ionic Liquid-Based Microemulsions and the Effect of n-Alcohols. *Ind. Eng. Chem. Res.* **2018**, *57*, 14846−14853.
(60) Li, Q.; Huang, X. Formation of 1-Butyl-3-methylimidazolium Bis (2-ethyl-1-hexyl) sulfosuccinate Stabilized Water-in-1-Butyl-3-methylimidazolium Bis (trifluoromethanesulfonyl) imide Microemulsion and the Effects of Additives. *J. Solution Chem.* **2017**, *46*, 1792−1804.
(61) Fife, T. H.; McMahon, D. M. Hydrolysis of bis(4-nitrophenyl) carbonate and the general base catalyzed hydrolysis of o-(4-nitrophenylene) carbonate. *J. Org. Chem.* **1970**, *35*, 3699−3704.
(62) El Seoud, O. A.; El Seoud, M. I.; Farah, J. P. Kinetics of the pH-Independent Hydrolysis of Bis (2, 4-dinitrophenyl) Carbonate in Acetonitrile−Water Mixtures: Effects of the Structure of the Solvent. *J. Org. Chem.* **1997**, *62*, 5928−5933.
(63) Garcia-Rio, L.; Leis, J. R.; Iglesias, E. Influence of water structure on solvolysis in water-in-oil microemulsions. *J. Phys. Chem. A* **1995**, *99*, 12318−12326.
(64) García-Río, L.; Leis, J. R.; Reigosa, C. Reactivity of Typical Solvolytic Reactions in SDS and TTABr Water-in-Oil Microemulsions. *J. Phys. Chem. B* **1997**, *101*, 5514−5520.
(65) Maitra, A. Determination of size parameters of water-Aerosol OT-oil reverse micelles from their nuclear magnetic resonance data. *J. Phys. Chem. A* **1984**, *88*, 5122−5125.
(66) Yu, Z. J.; Neuman, R. D. Giant rodlike reversed micelles. *J. Am. Chem. Soc.* **1994**, *116*, 4075−4076.
(67) Yu, Z. J.; Neuman, R. D. Reversed micellar solution-to-bicontinuous microemulsion transition in sodium bis (2-ethylhexyl) phosphate/n-heptane/water system. *Langmuir* **1995**, *11*, 1081−1086.
(68) Feng, K. I.; Schelly, Z. A. Equilibrium properties of crystallites and reverse micelles of sodium bis (2-ethylhexyl) phosphate in benzene. *J. Phys. Chem. A* **1995**, *99*, 17207−17211.
(69) Feng, K. I.; Schelly, Z. A. Electric birefringence dynamics of crystallites and reverse micelles of sodium bis (2-ethylhexyl) phosphate in benzene. *J. Phys. Chem. A* **1995**, *99*, 17212−17218.
(70) Quintana, S. S.; Falcone, R. D.; Silber, J. J.; Moyano, F.; Correa, N. M. On the characterization of NaDEHP/n-heptane nonaqueous reverse micelles: the effect of the polar solvent. *Phys. Chem. Chem. Phys.* **2015**, *17*, 7002−7011.
(71) Israelachvili, J. N.; Mitchell, D. J.; Ninham, B. W. Theory of self-assembly of hydrocarbon amphiphiles into micelles and bilayers. *J. Chem. Soc., Faraday Trans. 2* **1976**, *72*, 1525−1568.
(72) Mitchell, D. J.; Ninham, B. W. Micelles, vesicles and microemulsions. *J. Chem. Soc., Faraday Trans. 2* **1981**, *77*, 601−629.
(73) Tung, S. H.; Huang, Y. E.; Raghavan, S. R. A new reverse wormlike micellar system: mixtures of bile salt and lecithin in organic liquids. *J. Am. Chem. Soc.* **2006**, *128*, 5751−5756.
(74) Li, Q.; Li, T.; Wu, J.; Zhou, N. Comparative study on the structure of water in reverse micelles stabilized with sodium bis(2-

DOI: 10.1021/acs.langmuir.9b01083
Langmuir 2019, 35, 12744−12753

ethylhexyl) sulfosuccinate or sodium bis(2-ethylhexyl) phosphate in n-heptane. *J. Colloid Interface Sci.* **2000**, *229*, 298−302.
(75) Li, Q.; Li, T.; Wu, J. Comparative study on the structure of reverse micelles. 2. FT-IR, ^{1}H NMR, and electrical conductance of H_2O/AOT/NaDEHP/n-heptane systems. *J. Phys. Chem. B* **2000**, *104*, 9011−9016.
(76) Heatley, F. A ^{1}H nuclear magnetic resonance chemical-shift study of inverted microemulsions of aerosol OT in benzene and cyclohexane. Partitioning of water between hydrocarbon and aqueous phases. *J. Chem. Soc., Faraday Trans. 1* **1988**, *84*, 343−354.
(77) Stahla, M. L.; Baruah, B.; James, D. M.; Johnson, M. D.; Levinger, N. E.; Crans, D. C. ^{1}H NMR studies of aerosol-OT reverse micelles with alkali and magnesium counterions: Preparation and analysis of MAOTs. *Langmuir* **2008**, *24*, 6027−6035.
(78) Fernández, E.; García-Río, L.; Parajó, M.; Rodriguez-Dafonte, P. Influence of changes in water properties on reactivity in strongly acidic microemulsions. *J. Phys. Chem. B* **2007**, *111*, 5193−5203.
(79) Blach, D.; Correa, N. M.; Silber, J. J.; Falcone, R. D. Interfacial water with special electron donor properties: Effect of water-surfactant interaction in confined reversed micellar environments and its influence on the coordination chemistry of a copper complex. *J. Colloid Interface Sci.* **2011**, *355*, 124−130.
(80) McNeil, R.; Thomas, J. K. Benzylhexadecyldimethylammonium chloride in microemulsions and micelles. *J. Colloid Interface Sci.* **1981**, *83*, 57−65.
(81) Blach, D.; Silber, J. J.; Correa, N. M.; Falcone, R. D. Electron donor ionic liquids entrapped in anionic and cationic reverse micelles. Effects of the interface on the ionic liquid-surfactant interactions. *Phys. Chem. Chem. Phys.* **2013**, *15*, 16746−16757.
(82) Headley, A. D.; Jackson, N. M. The effect of the anion on the chemical shifts of the aromatic hydrogen atoms of liquid 1-butyl-3-methylimidazolium salts. *J. Phys. Org. Chem.* **2002**, *15*, 52−55.
(83) Menger, F. M.; Venkatasubban, K. S. Proton inventory study of a water-catalyzed hydrolysis. *J. Org. Chem* **1976**, *41*, 1868−1870.
(84) Fife, T. H.; McMahon, D. M. Acid-and water-catalyzed hydrolysis of p-nitrophenyl esters. *J. Am. Chem. Soc.* **1969**, *91*, 7481−7485.
(85) Campos-Rey, P.; Cabaleiro-Lago, C.; Hervés, P. Promoting Mechanistic Changes: Solvolysis of Benzoyl Halides in Nonionic Microemulsions. *J. Phys. Chem. B* **2009**, *113*, 11921−11927.

DOI: 10.1021/acs.langmuir.9b01083
Langmuir 2019, 35, 12744−12753